Optical transport, lifting and trapping of micro-particles by planar waveguides

Øystein Ivar Helle,* Balpreet Singh Ahluwalia and Olav Gaute Hellesø

Department of Physics and Technology, University of Tromsø, 9037 Tromsø, Norway

*oystein.i.helle@uit.no

Abstract: Optical waveguides can be used to trap and transport micro-particles. The particles are held close to the waveguide surface by the evanescent field and propelled forward. We propose a new technique to lift and trap particles above the surface of the waveguides. This is made possible by a gap between two opposing, planar waveguides. The field emitted from each of the waveguide ends diverge fast, away from the substrate and into the cover-medium. By combining two fields propagating at an angle upwards and coming from opposite sides of a gap, particles can be stably lifted and trapped at the crossing of the two fields. Thus, particles are transported by waveguides leading to a gap, where they are lifted away from the substrate and trapped. The experiments are supported by numerical simulations of the forces on the micro-particles. Fluorescence imaging is used to track the particles in 3D with a precision of 50 nm.

OCIS codes: (140.7010) Laser trapping; (230.3120) Integrated optics devices; (350.4855) Optical tweezers or optical manipulation.

References and links

1. G. Sagvolden, I. Giaever, E. O. Pettersen, and J. Feder, "Cell adhesion force microscopy," Proceedings of the National Academy of Sciences **96**, 471–476 (1999).
2. G. W. Francis, L. R. Fisher, R. A. Gamble, and D. Gingell, "Direct measurement of cell detachment force on single cells using a new electromechanical method," J. Cell. Sci. **87 (Pt 4)**, 519–523 (1987).
3. X. Wang, S. Chen, M. Kong, Z. Wang, K. D. Costa, R. A. Li, and D. Sun, "Enhanced cell sorting and manipulation with combined optical tweezer and microfluidic chip technologies," Lab Chip **11**, 3656–3662 (2011).
4. S. Kawata and T. Tani, "Optically driven mie particles in an evanescent field along a channeled waveguide," Opt. Lett. **21**, 1768–1770 (1996).
5. B. S. Schmidt, A. H. Yang, D. Erickson, and M. Lipson, "Optofluidic trapping and transport on solid core waveguides within a microfluidic device," Opt. Express **15**, 14322–14334 (2007).
6. K. Grujic, O. Hellesø, J. Wilkinson, and J. Hole, "Optical propulsion of microspheres along a channel waveguide produced by cs+ ion-exchange in glass," Opt. Commun. **239**, 227 – 235 (2004).
7. G. Brambilla, G. S. Murugan, J. S. Wilkinson, and D. J. Richardson, "Optical manipulation of microspheres along a subwavelength optical wire," Opt. Lett. **32**, 3041–3043 (2007).
8. K. Grujic and O. G. Hellesø, "Dielectric microsphere manipulation and chain assembly by counter-propagating waves in a channel waveguide," Opt. Express **15**, 6470–6477 (2007).
9. P. Løvhaugen, B. S. Ahluwalia, T. R. Huser, and O. G. Hellesø, "Serial raman spectroscopy of particles trapped on a waveguide," Opt. Express **21**, 2964–2970 (2013).
10. O. G. Hellesø, P. Løvhaugen, A. Z. Subramanian, J. S. Wilkinson, and B. S. Ahluwalia, "Surface transport and stable trapping of particles and cells by an optical waveguide loop," Lab Chip **12**, 3436–3440 (2012).
11. M. Boerkamp, T. van Leest, J. Heldens, A. Leinse, M. Hoekman, R. Heideman, and J. Caro, "On-chip optical trapping and raman spectroscopy using a triplex dual-waveguide trap," Opt. Express **22**, 30528–30537 (2014).
12. A. Ashkin and J. M. Dziedzic, "Optical levitation by radiation pressure," Appl. Phys. Lett. **19**, 283–285 (1971).
13. V. Garcés-Chávez, D. Roskey, M. D. Summers, H. Melville, D. McGloin, E. M. Wright, and K. Dholakia, "Optical levitation in a bessel light beam," Appl. Phys. Lett. **85**, 4001–4003 (2004).

#229371 - $15.00 USD Received 10 Dec 2014; revised 9 Feb 2015; accepted 10 Feb 2015; published 3 Mar 2015

14. G. A. Swartzlander, T. J. Peterson, A. B. Artusio-Glimpse, and A. D. Raisanen, "Stable optical lift," Nat. Photon. **5**, 48–51 (2011).
15. M. Speidel, A. Jonáš, and E.-L. Florin, "Three-dimensional tracking of fluorescent nanoparticles with subnanometer precision by use of off-focus imaging," Opt. Lett. **28**, 69–71 (2003).
16. B. Ahluwalia, A. Subramanian, O. Hellsø, N. Perney, N. Sessions, and J. Wilkinson, "Fabrication of submicrometer high refractive index tantalum pentoxide waveguides for optical propulsion of microparticles," IEEE Photon. Technol. Lett. **21**, 1408–1410 (2009).
17. R. Parthasarathy, "Rapid, accurate particle tracking by calculation of radial symmetry centers," Nat. Meth. **9**, 724–726 (2012).
18. E. Billauer, "Peakdet, peak detecting algorithm," http://www.billauer.co.il/peakdet.html, accessed 14/5/14 .
19. J. Hole, J. Wilkinson, K. Grujic, and O. Hellesø, "Velocity distribution of gold nanoparticles trapped on an optical waveguide," Opt. Express **13**, 3896–3901 (2005).
20. T. Tanaka and S. Yamamoto, "Optically induced meandering mie particles driven by the beat of coupled guided modes produced in a multimode waveguide," Jpn. J. Appl. Phys. **41**, L260 (2002).
21. H. Deschout, K. Raemdonck, S. Stremersch, P. Maoddi, G. Mernier, P. Renaud, S. Jiguet, A. Hendrix, M. Bracke, R. Van den Broecke, M. Röding, M. Rudemo, J. Demeester, S. De Smedt, F. Strubbe, K. Neyts, and K. Braeckmans, "On-chip light sheet illumination enables diagnostic size and concentration measurements of membrane vesicles in biofluids," Nanoscale **6**, 1741–1747 (2014).
22. J. N. George, R. I. Weed, and C. F. Reed, "Adhesion of human erythrocytes to glass: The nature of the interaction and the effect of serum and plasma," J. Cell. Physiol. **77**, 51–59 (1971).

1. Introduction

For lab-on-a-chip devices, a method that can deliver particles to a precise location and lift them away from the surface would be useful, e.g to analyze a single cell or to expose it to a special chemical or biological environment. By lifting the particle away from the surface, unwanted chemical, optical and electrostatic/adhesive [1,2] effects related to the substrate can be avoided. For moving large numbers of particles, microfluidics is the appropriate technique [3]. Waveguide propulsion is a promising technique for manipulating a few or single micro-particles [4–8]. Particles are attracted towards the waveguide surface by the evanescent field of the waveguide. The radiation pressure continuously push the particles forward. Raman-spectroscopy has been used to characterize particles propelled along a waveguide [9]. Lifting the particles up would avoid recording the Raman-spectra of the substrate.

Waveguides are compatible with lab-on-a-chip devices, but move particles rather than trap them, and press them down to the surface, rather than lift them. To stop particles, it has previously been proposed to use counter-propagating light in a straight waveguide [8]. The method can trap particles at any location along the waveguide, but with limited precision. Recently, a waveguide loop with an intentional gap was used to propel particles towards the gap and stably trap the particles in the gap [10]. Waveguide loops with gap separation of 2-30 μm were demonstrated to precisely trap micro-spheres of different sizes and also red blood cells. The waveguide loop with gap can also be combined with a transverse microfluidic chamber, for delivering particles to the gap [11]. This approach, although it is fast, it is less predictable in which particles are trapped.

As for lifting a particle, the first results on optical levitation were reported by Askhin [12] in 1971. The particles were levitated by a single vertically directed Gaussian beam, and the particles were shown to stably settle at the force equilibrium with gravity. Many reports have since been made on optical levitation by Gaussian beams and particles have also been levitated using a zero-order Bessel beam [13]. Another, more recent approach to vertically lift microparticles in water, has been investigated by Swartzlander et.al [14]. A non-symmetrical rod placed in a uniform stream of light was seen to experience a force transverse to the direction of beam propagation, in analogy with aerodynamic lift. The previous approaches to levitation have relied on bulk optics, which is difficult or impossible to combine with a lab-on-a-chip.

The evanescent field of a waveguide attracts the particle towards the surface, and one or more free-space beams thus have to be generated to lift a particle away from the surface. Two free-

#229371 - $15.00 USD Received 10 Dec 2014; revised 9 Feb 2015; accepted 10 Feb 2015; published 3 Mar 2015

space beams can be created by an intentional gap in a waveguide loop [10]. It will be shown with simulations that the field from the end of a waveguide divides into two parts, with one part going downwards, into the substrate, and one part going upwards, into the cover medium and away from the substrate. By using a sufficiently wide gap, here 10 μm wide, the fields have enough space to diverge away from the substrate before they cross each other, and a particle can be lifted and trapped in three dimensions at the crossing of the two diverging fields. Whereas the evanescent field has been used for pulling particles down to the surface of the waveguide, we thus propose a new technique in which the diverging field at the end of waveguides is used to lift and trap micro-particles above the planar waveguide surface.

In order to experimentally verify that a particle is lifted, it is necessary to track it in three dimensions. Speidel et al. [15] have proposed using off-focus imaging of nano-particles to determine the axial position. We have adapted this method for tracking micro-particles, and combined with optical trapping we can track the particle displacement in three-dimensions. The method is applied to track micro-particles (2 μm diameter) as they are propelled along a straight waveguide, and when they are optically lifted in a 10 μm wide gap.

2. Waveguides and experimental setup

Waveguides with a tantalum pentoxide (Ta_2O_5) core were fabricated on oxidized silicon substrates. Further detail can be found in [16]. Tantalum pentoxide has a high refractive index (2.15 at wavelength 1070 nm), which, together with the small cross-section of the waveguides (180 nm thick by 1.3 μm wide), ensures tight confinement laterally, a strong evanescent field and single-mode operation for this wavelength. The input waveguide is 2 μm wide and tapers down to 1.3 μm to provide good input coupling, and to ensure single mode operation in the loop. The small cross-section also gives large divergence of the field at the end of a waveguide, as will be shown in the next section. The waveguide loop, which is used for sending light to the gap, is shown in Fig. 1(a). Figure 1(b) shows a SEM image of the gap used for trapping, and Figs. 1(c) and 1(d) shows schematic diagrams of the gap. A 1070 nm Ytterbium (IPG ylm-1070-lp) fiber-coupled laser delivered 400 mW-600 mW to the input facet of the waveguides.

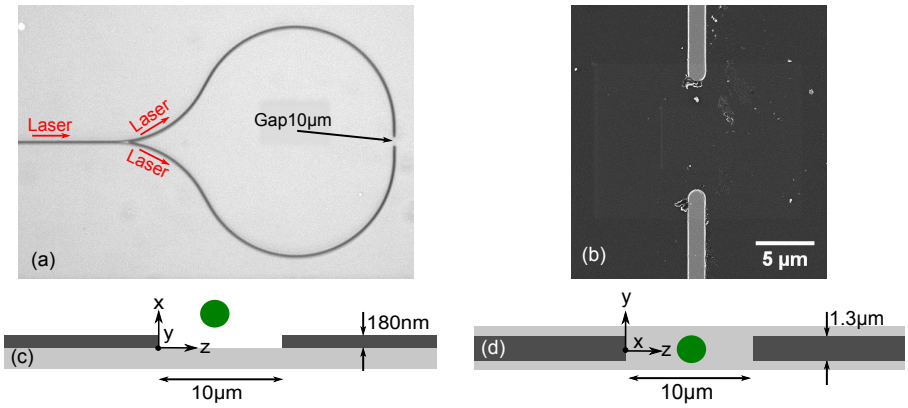

Fig. 1. (a) Optical bright field image of a waveguide loop with gap. Laser light is coupled into the straight part and divides into the two arms. (b) SEM image of the gap, seen from the top. (c) Schematic diagram, side-view, of particle in the gap between two waveguide ends (not to scale). The particle is lifted as it enters the gap. (d) Schematic diagram of the gap, top-view.

To couple light into the (input) waveguide, the laser light is focused on the waveguide input facet using an IR-coated objective lens (Nachet 100X, NA 0.8). Both the objective lens and

#229371 - $15.00 USD Received 10 Dec 2014; revised 9 Feb 2015; accepted 10 Feb 2015; published 3 Mar 2015

the waveguide chip are positioned by piezoelectric translation stages to ensure good coupling. The waveguide chip is held by vacuum suction to minimize mechanically induced noise. A weak solution of fluorescent polystyrene particles and distilled water is held in a PDMS microchamber on top of the waveguide chip. Commercial, monodisperse particles were used (Bangs Labs, diameter 2 μm, density 1.05 g/cm^3). A microscope is used to observe the particles from the top. To excite fluorescence, 532 nm laser light is sent through the microscope, illuminating the sample from the top. A band-pass filter removes other wavelengths and transmits the fluorescent light to a CCD-camera on the microscope. The CCD-camera is used to record real-time movies of the trapped particles. The individual movie frames are analyzed using an algorithm (Matlab) to track the motion of the particles in three dimensions, as will be described in section 4.

3. Simulations

The electromagnetic field distribution between the waveguide ends was simulated with Comsol Multiphysics (version 4.4), which is based on the finite element method. To find the optical forces on a polystyrene sphere, the field distribution was used to integrate Maxwell's stress tensor over the surface of the sphere. The sphere was moved to a number of positions in the model (xz-plane) and the field and forces calculated for each position. Seven mesh-points per wavelength were used for the waveguide core and the surface of the sphere, with a less dense mesh elsewhere. Perfectly matched layers (PML) were used on all sides of the model, except the symmetry plane (y = 0), which was set to be a perfect electrical conductor (PEC). The model was checked for stability regarding mesh and reflections from the boundaries. Simulations were done for the symmetric case only, with the sphere in the xz-plane, which makes it possible to simulate only half of the model. Geometrical and optical parameters were the same as for the experiments, with refractive indices of 1.33 for water, 2.15 for Ta2O5, 1.45 for silica and 1.59 for polystyrene. All simulations have been done for a 10 μm wide gap. The waveguide ends were taken to be rounded, as seen in Fig. 1(b). The power from each waveguide end was set to 1 mW. Note that all forces are proportional with the input power.

By intentionally ending the waveguide, the guided light inside the waveguide can be converted into a freely propagating field. The field distribution of the light escaping the end facet of the waveguide is simulated and shown in Fig. 2(a). When light is present in only one of the waveguides, the emitted field shows a large divergence angle in x-direction. The field distribution is continuous across the substrate - water interface close to the waveguide end. Further away from the waveguide end, light is divided in two parts, with one part propagating downwards, into the substrate, and one part propagating upwards, into the water. As the refractive index of the oxidized substrate (i.e. silica) is higher than that of water (1.46 vs. 1.33), more light is emitted into the substrate than into the water. The light propagating upwards has a large angular distribution, with a maximum at approximately 25 degrees with the substrate - water interface. With light emitted from both waveguides, Fig. 2(b), an interference pattern is present in almost the entire model. Due to symmetry, equal power is going towards the left and towards the right in the middle of the gap, giving a straight interference fringe and zero force in the z-direction. The end of a waveguide gives some reflection back into the waveguide, and interference can also be seen inside the waveguides, with the periodicity given by the effective index of the waveguide (n_{eff} = 1.69, giving $\lambda/2n_{eff}$ = 317 nm).

#229371 - $15.00 USD Received 10 Dec 2014; revised 9 Feb 2015; accepted 10 Feb 2015; published 3 Mar 2015

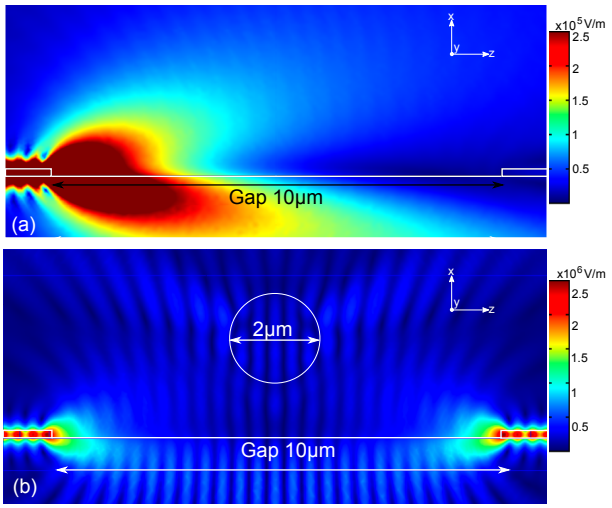

Fig. 2. Simulation of the field distribution in a 10 μm wide gap. The norm of the electrical field is shown. (a) Light emitted from a (single) waveguide end has a large angular distribution (range of colors is compressed to visualize the emittance angle). (b) Light emitted from two waveguide ends interfere, creating stable trapping for particles at a distance above the waveguide chip.

Figures 3(a)–3(c) shows the optical forces acting on a polystyrene sphere with 2 μm diameter in a 10 μm wide gap. The forces are shown for various positions relative to the end of the left waveguide (z = 0). For a particle close to the surface of the substrate (x = 0), the vertical force $F_x(z)$ is negative near the waveguide ends, thus particles near the waveguide ends will be pulled downwards to the substrate. Towards the middle of the gap, $F_x(z)$ turns positive. The force $F_z(z)$ along the gap has a large positive value close to the left waveguide and a large negative value close to the right waveguide, in both cases pushing the particle towards the center of the gap. The simulations thus predict that particles will be pushed towards the middle of the gap, where they will be pushed upwards. The exact trapping position (along the z-axis) depends on the interaction of the sphere with the interference fringes. In the middle of the gap (z = 3 - 7 μm), $F_z(z)$ is seen to oscillate around zero, creating several stable trapping locations along the z-direction. A stable trapping location z_s is identified as a point where a restoring force is present, i.e $F_z(z_s - \varepsilon) > 0$ and $F_z(z_s + \varepsilon) < 0$ for an interval ε in the neighborhood of z_s. To confirm if the particle is stably trapped along x, it is necessary to compute the forces on the particle for various positions on the x-axis. For a particle in the center of the gap, z = 5 μm, Fig. 3(c) shows that the vertical force $F_x(x)$ offer two stable trapping locations, for x = 1.2 μm and x = 3.1 μm . As this is in the center of the gap, $F_z(z)$ is also zero for these locations. The simulations thus predict that a particle can be trapped in the center of the gap and levitated 1.2 or 3.1 μm above the substrate.

Symmetry gives that for all positions studied, which are in the xz-plane with $y = 0$, the transverse force $F_y = 0$. As the interference fringes extend several micrometers upwards, there are a number of trapping positions in the xz-plane where both $F_x = 0$ and $F_z = 0$. Figure 3(b) shows approximately 10 trapping positions along the z-axis for x = 0, while Fig. 3(c) shows two along the x-axis for z = 5 μm, giving a total of 20 in the xz-plane. A complete survey of these has not been carried out, but they will largely follow the interference pattern in Fig. 2(b).

#229371 - $15.00 USD Received 10 Dec 2014; revised 9 Feb 2015; accepted 10 Feb 2015; published 3 Mar 2015

If the phase of the field changes at one waveguide end relative to the other, the interference pattern will move accordingly within the period of the interference fringes ($\lambda/2$). If the field amplitude at one waveguide end changes, the visibility will be reduced, the trapping by the interference fringes become weaker and the centre of the interference pattern will shift along the z-axis according to the ratio of the two amplitudes. In addition, experimentally, the exact positions of the fringes and thus the trapping locations, depend on the geometrical parameters of the waveguide end-facets (width, angle, rounding, thickness, defects, etc). The simulations thus predict lifting of the particle along the x-axis and trapping within the central part of the gap, but cannot predict the exact trapping location.

4. 3D tracking of fluorescent particles

A method to track the movement in x-direction of a particle based on off-focus imaging was used [15]. The method exploits the diffraction rings created when imaging a particle out of focus. As the distance from focus is altered, the diffraction pattern keeps its symmetry, but the radii of the diffraction rings change. The outermost diffraction ring is the brightest, and a calibration is first done to find the relationship between the radius of the outermost diffraction ring and the distance from focus. Second, the inverse relationship is used when tracking the axial position of particles. The center of the 2D intensity distribution is found [17] and the 2D image is transformed into a 1D intensity distribution by averaging the intensity of concentric circles around the center of the 2D image. A peak detecting algorithm [18] is used to give an estimate for the radius of the diffraction ring. Furthermore, a 4th-order polynomial is fitted to the peak to reduce the influence of noise and improve the estimate for the radius. Figure 4(a) show a 2D-intensity distribution and Fig. 4(b) give the 1D-intensity distribution and radii estimate.

For the calibration, 2 μm fluorescent particles were immobilized by evaporating a water-particle mixture on top of the waveguide, and imaged with a fluorescence microscope. A series of images were acquired, and for each image the distance from focus was changed by 1 μm . The radius of the diffraction ring was measured for each image acquired, giving the calibration curve shown in Fig. 4(c). The radius of the diffraction ring is seen to decrease linearly as the microscope objective is moved down towards focus. Far away from focus (displacement < 5 μm in Fig. 4(c), the diffraction ring had very low intensity and the radius was not correctly calculated. The radius for these points thus deviates from the linear relationship. Close to focus (displacement > 35 μm), the diffraction ring merge into a single spot and the radius cannot be calculated precisely. For the linear range (displacement 5 to 33 μm in Fig. 4), a straight line is fitted to the measured radii. The calibration was repeated 10 times and the average slope of the fitted straight lines was found. The inverse slope, which is used for tracking, was 184 ± 6 nm/pixel with a 50x objective. The microscope was also moved in the zy-plane with fixed displacements to find the relationship between zy-movement and pixels. The resulting calibration factor was found to be 66 ± 1 nm/pixel.

5. Results

5.1. Tracking of immobilized particles

To test the tracking method, it was used on immobilized particles and on particles propelled along a waveguide. Immobilized particles were imaged out-of-focus over time. The experiment was repeated five times and 20 seconds long movies acquired each time. The average standard deviation for the motion along x of an immobilized particle was $\sigma_x = 50$ nm. This measured noise is a combination of noise associated with the experimental set-up (mechanical vibrations and drift, illumination, photo-bleaching and camera noise).

#229371 - $15.00 USD Received 10 Dec 2014; revised 9 Feb 2015; accepted 10 Feb 2015; published 3 Mar 2015

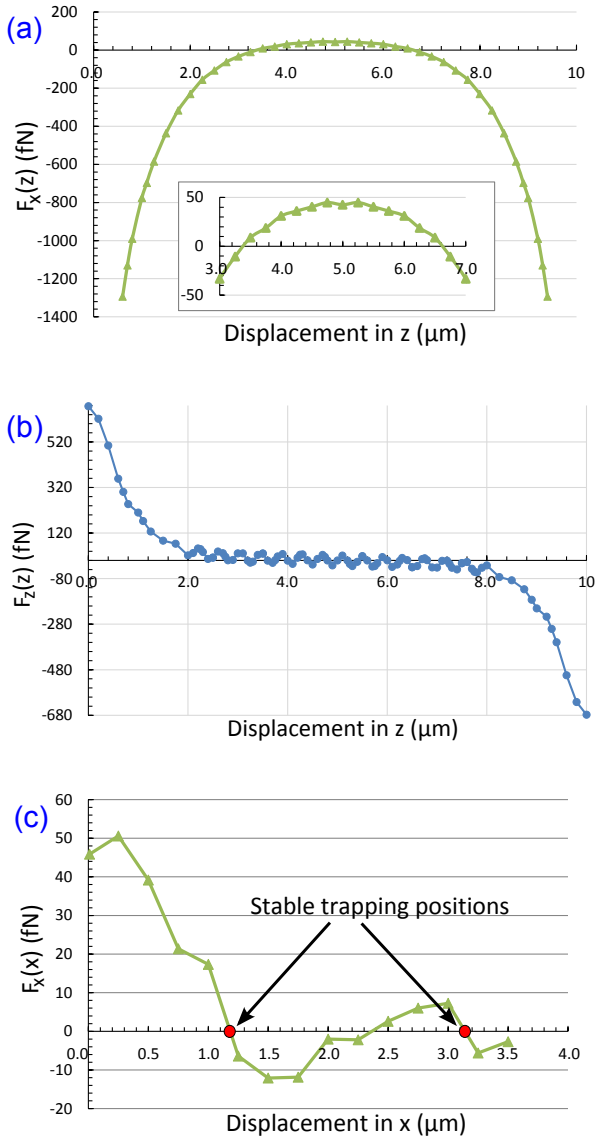

Fig. 3. Calculated forces acting on a 2 μm diameter sphere in a 10 μm wide gap. (a) $F_x(z)$ becomes positive some distance into the gap. Particles are thus expected to levitate as they approach the center of the gap. (b) $F_z(z)$ push particles towards the center of the gap. In the middle of the gap, $F_z(z)$ oscillates around zero, creating several stable trapping locations. (c) In the center of the gap (z = 5 μm), $F_x(x)$ is seen to offer two stable locations where a restoring force is present.

5.2. Tracking of particles on top of straight, planar waveguides

Micro-particles were trapped and propelled along a 2 μm wide, straight waveguide. As the particles are pulled down to the waveguide surface by the evanescent field and the waveguide is planar, the particles should move along z-direction with very little movement in x-direction. An

#229371 - $15.00 USD Received 10 Dec 2014; revised 9 Feb 2015; accepted 10 Feb 2015; published 3 Mar 2015

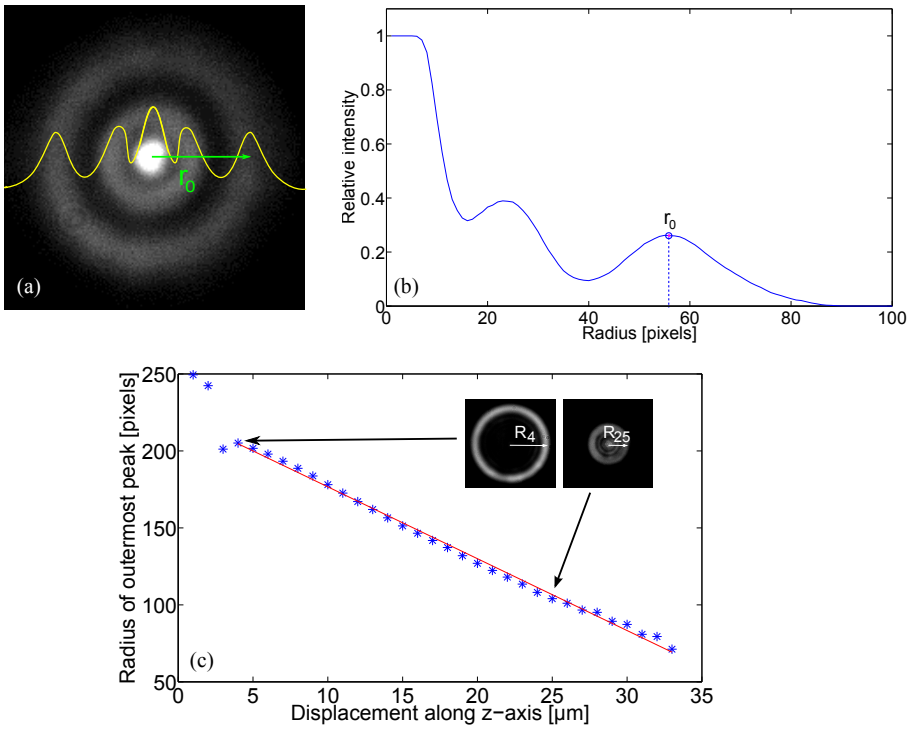

Fig. 4. (a) 2D image of out-of-focus particle. (b) 1D intensity distribution of particle in (a) and the final estimate of the radius. (c) Calibration curve showing the linear relationship between radius of the outermost diffraction ring and the distance from focus. The calibration curve is made by finding the radius of the outermost diffraction ring for a series of images, with the distance from focus decreased by 1 μm between each image.

out-of-focus movie was recorded of the particles as they moved along the waveguide (see Media 1). The tracking algorithm was used to find the position along the x-axis of single particles for each frame in the movie. Figure 5(a) shows 3 selected frames from Media 1, and Fig. 5(b) shows the result of tracking the particle in x-direction. The standard deviation of the motion in x-direction of 10 different particles ranged from 43 to 71 nm, with an average of $\sigma_x = 55$ nm. This is comparable to the noise found for an immobilized particle ($\sigma_x = 50$ nm). The precision of the method is thus sufficient to measure a separation in the micrometer-range between the particle and the waveguide, as will be shown in the next section. For a particle propelled on a waveguide, the largest deviations were caused by non-uniform illumination, making some frames appear brighter (see frame 28 in Fig.5). This contribution to noise is not present when testing the method on immobilized particles.

The tracking along the x-axis confirms that the particles are moving within the evanescent field, which has a decay-length (1/e) of 160 nm according to the simulations. The particle was also tracked in the y-direction, as shown in Fig.5(c). Meandering of the trapped particle was observed as the particle moved along the waveguide. As this 2 μm wide waveguide was multimode, the meandering is caused by multimode interference [19, 20]. In the loop-section, the waveguides were 1.3 μm wide and single-mode. No meandering was thus observed on the loop.

#229371 - $15.00 USD Received 10 Dec 2014; revised 9 Feb 2015; accepted 10 Feb 2015; published 3 Mar 2015

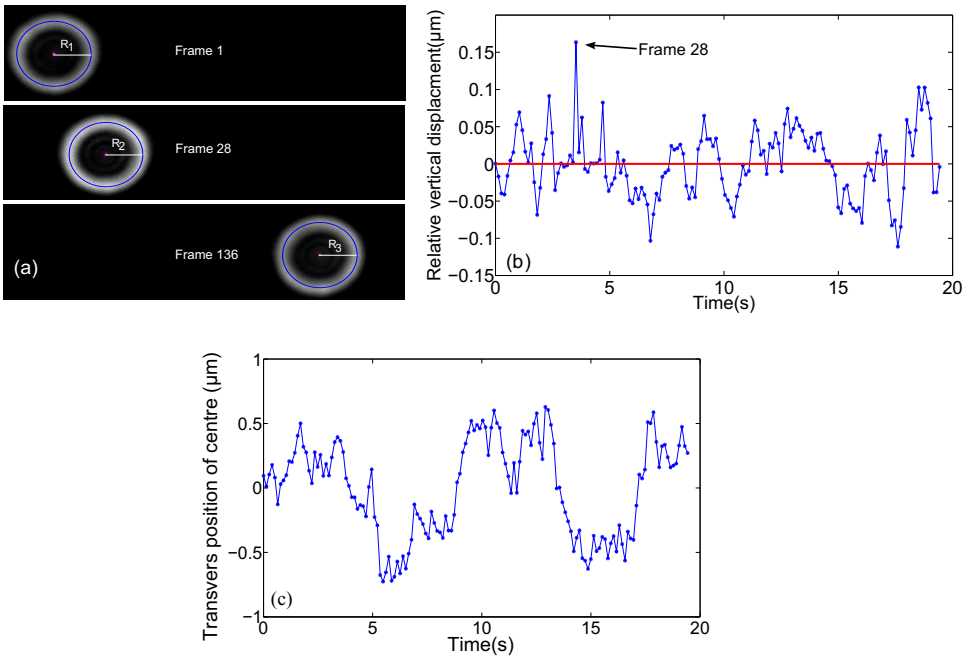

Fig. 5. A particle propelling along a straight waveguide (see Media 1) is tracked in the x-direction. (a) Some frames from the movie showing the diffraction rings and the radius found by the tracking algorithm. (b) Result of the x-direction tracking, with a standard deviation of 45 nm. The particle moved 53 μm along the waveguide during the 20 second interval.(c) Result of tracking the center of the same particle in the y-direction. Optical meandering is observed.

5.3. Lifting and trapping particles in a gap.

To experimentally demonstrate that a 10 μm wide gap between planar waveguides can lift and trap particles, 2 μm polystyrene particles were used, as for the simulations. The particles are captured by the evanescent field and transported to the gap by the arms of the loop. Movies were recorded of single particles, starting when a particle propelled along one of the two waveguides and approaching the loop. The recording was stopped when the particle had been trapped in the gap for a while (10-20 s), and the laser light had been switched off. The movies were analyzed with the tracking algorithm to find the position in 3D. Figure 6 shows two frames from a movie (see Media 2) of a particle being trapped in the gap. The result of tracking both in x- and z-direction can be seen in Fig. 7. For the first few seconds ($t < 4.5s$) in Fig. 7 (see associated movie), the radius of the diffraction ring remains almost constant (no movement along x-axis) as the particle is held close to the waveguide surface by the evanescent field. The radius of the diffraction ring decreases as the particle enters the gap, corresponding to a displacement along the x-axis. The particle is lifted up when it enters the gap, and stays trapped at x = 2.2 μm relative to the surface of the waveguides. Adding 180 nm for the waveguide height, gives that the particles are lifted 2.4 μm above the waveguide chip (i.e. substrate), with a standard deviation of 0.5 μm . The experiment was repeated six times (i.e. for six particles), giving an average lift of 1.1 μm above the waveguide chip. This corresponds well with trapping at the lowest stable trapping location predicted by the simulations (1.2 μm). However, the relatively large range of the measured lift, 0.5-2.4 μm, may indicate that a particle can be trapped at both trapping locations given by the simulations (1.2 and 3.1 μm). In addition, thermal noise, flow

#229371 - $15.00 USD Received 10 Dec 2014; revised 9 Feb 2015; accepted 10 Feb 2015; published 3 Mar 2015

in the cell or a tilt of the waveguide facet may explain the variation in the lift and deviations from the simulations.

The z-position is approximately linear with time as the particle propels along one of the arms of the waveguide loop ($t < 4.5s$), indicating a constant propulsion speed (see Fig. 7). As the particle leaves the waveguide and enters the gap ($t \approx 4.5s$), there is a sudden increase in z-position, indicating a higher propulsion speed (see Media 2). Finally, the particle comes to rest as it is trapped in the gap. For this particular experiment, the trapping location was z= 6.0 μm from the waveguide end. The average trapping distance for the six experiments was 6.5 μm from the waveguide end. The deviation from the center of the gap (i.e. 5 μm) is most likely due to slightly higher power coming from one waveguide end than from the other.

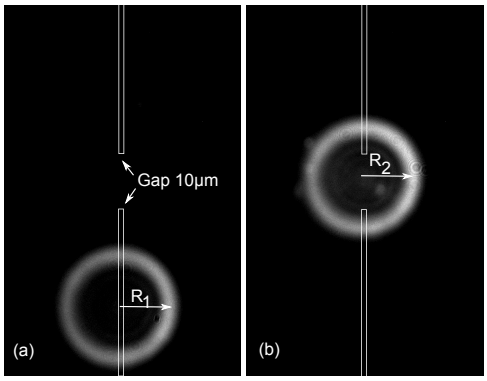

Fig. 6. Fluorescent particle trapped in a gap (see Media 2). (a) The particle is on the waveguide arm, with diffraction ring with radius R_1. (b) The particle is trapped in the gap, with radius R_2 for the diffraction ring. As $R_2 < R_1$, the particle is lifted.

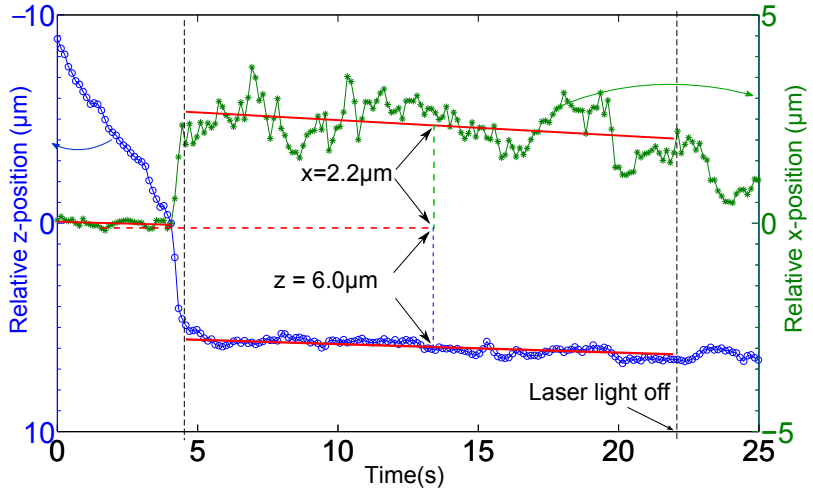

Fig. 7. Tracking of a 2 μm diameter particle in a 10 μm wide gap, both in x- and z-direction. The particle is lifted 2.2 μm relative to the waveguide and 2.4 μm relative to the surface of the waveguide chip. In z-direction, the particle is trapped on an average 6.0 μm from the waveguide end (i.e. 4.0 μm from the other waveguide). Axis for z-position has been reversed for clarity.

#229371 - $15.00 USD Received 10 Dec 2014; revised 9 Feb 2015; accepted 10 Feb 2015; published 3 Mar 2015

Brownian motion cause the particles to move within the trap. The average standard deviation in position was σ_x =0.31 μm, σ_y =0.30 μm and σ_z =0.25 μm. Particles are thus trapped most tightly along the z-axis, with σ_z =0.25 μm indicating trapping within one or two interference fringes (period $\lambda/2n$ =402 nm). Figures 8(a)–8(c) shows the histograms of the position of the particle tracked in Media 2, and the fitted gaussian.

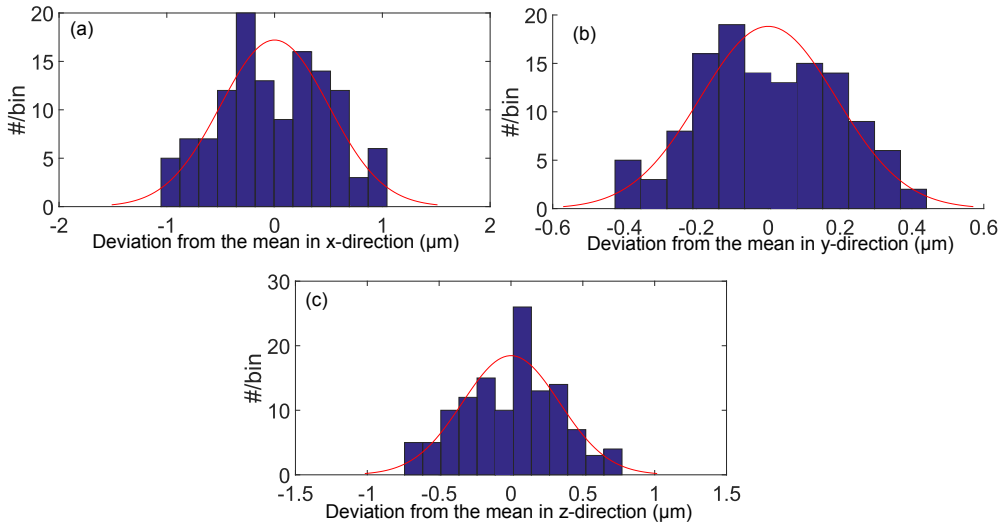

Fig. 8. Histogram of the position of the trapped particle (see Media 2) trapped in the gap with fitted gaussian, in (a) x-, (b) y- and (c) z-direction. The position is given as the deviation from the mean when trapped in the gap.

6. Discussion and conclusion

The arms of a waveguide loop were used to move micro-particles towards a 10 μm wide gap between the opposing waveguide ends. The particles were levitated and stably trapped in the gap. For six particles measured, the lift ranged from 0.5 to 2.4 μm, with an average of 1.1 μm above the surface of the chip. Simulations predicted two stable positions along the x-axis, at x=1.2 μm and x=3.1 μm, for a particle trapped in the center of the gap. Experimentally, particles were trapped at z=6 μm from one of the waveguides, thus away from the center of the gap. Due to the interference of the two fields, there are a number of stable trapping positions along the z-axis. These were found with simulations for x = 0 (along the surface of the substrate), but a complete mapping of all the stable trapping positions in the xz-plane was not done. It is possible that, experimentally, particles are trapped at, or moving between, these positions in the xz-plane and possibly also moving to stable positions with $y \neq 0$. Experimentally, several effects will contribute to variations in the trapping position and trapping at positions different from those predicted by the simulations. These effects include Brownian motion, flow in the cell, unequal power in the two arms of the waveguide loop and imperfections of the waveguide end-faces.

The tracking method is based on off-focus fluorescence imaging of the outer diffraction ring of a particle. Changes in the illumination, photo-bleaching, image noise and mechanical vibrations in the set-up will contribute to noise in the tracking. Immobilized particles and particles moving along planar waveguides were tracked to test the method, giving average standard deviations for the x-position of 50 and 55 nm, respectively. The tracking uncertainty is thus significantly smaller than the measured lift and also smaller than the variation in the trapping

#229371 - $15.00 USD Received 10 Dec 2014; revised 9 Feb 2015; accepted 10 Feb 2015; published 3 Mar 2015

position, which was found to be σ_x =0.31 μm, σ_y =0.3 μm and σ_z =0.25 μm (average std. dev. for six trapped particles).

The width of the gap strongly influences the lift and the trapping, with a small gap giving stronger trapping, but less or no lift. The cross-section and the refractive index of the waveguides will influence the divergence of the field from the end of the waveguide, and thus the trapping in the gap. Slightly larger waveguides (2-3 μm wide) would reduce the divergence along z-direction and thus give tighter trapping along the y-axis. By changing the shape of the waveguide ends it might be possible to steer the two opposing beams and improve the trapping, e.g. by making lens-shaped ends or change the angle of the end-facet.

The diverging light fields between the waveguide gap can also combine waveguide trapping with on-chip fluorescence imaging [21]. Lifting particles away from the surface of the waveguide might improve the signal-to-noise ratio when analyzing biological samples. The biological samples are often kept in physiological saline solution, typically phosphate buffer solution (PBS). The salt content of the saline medium generate electrostatic adhesive forces between cell and the surface [1, 2, 22], which is much higher than the optical forces typically imparted in optical trapping. Thus, even a small separation of a few micrometers will be useful to reduce such adhesive forces.

The waveguide loop with a gap gives new functionality to particle manipulation, as it can transport, trap and levitate particles at a pre-determined location. The proposed method is compatible with microfluidics and can be integrated in a lab-on-a-chip. If combined with additional waveguides and waveguide sensors, the system may enable both analyzing and sorting of microparticles.

#229371 - $15.00 USD Received 10 Dec 2014; revised 9 Feb 2015; accepted 10 Feb 2015; published 3 Mar 2015